Synthesis of Carboxy ATTO 647N Using Redox Cycling for Xanthone Access

James L. Bachman,[†] Cyprian I. Pavlich,[†] Alexander J. Boley,[†] Edward M. Marcotte,[‡] and Eric V. Anslyn*,[†] (ORCID)

[†]Department of Chemistry, The University of Texas at Austin, Austin, Texas 78712, United States
[‡]Department of Molecular Biosciences, The University of Texas at Austin, Austin, Texas 78712, United States

S *Supporting Information*

ABSTRACT: A synthesis of the carbopyronine dye Carboxy ATTO 647N from simple materials is reported. This route proceeds in 11 forward steps from 3-bromoaniline with the key xanthone intermediate formed using a new oxidation methodology. The step utilizes an oxidation cycle with base, water, iodine, and more than doubles the yield of the standard permanganate oxidation methodology, accessing gram-scale quantities of this late-stage product. From this, Carboxy ATTO 647N was prepared in only four additional steps. This facile route to a complex fluorophore is expected to enable further studies in fluorescence imaging.
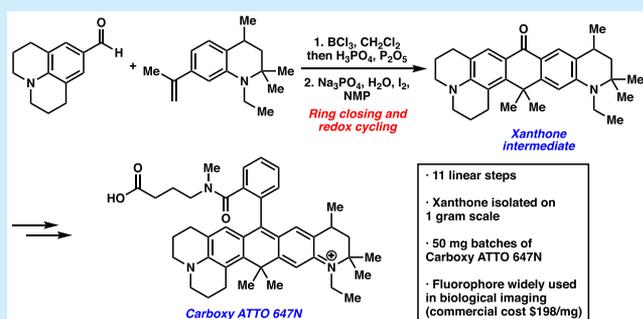
Far-red and near-infrared (IR) emitting fluorophores are invaluable tools in biological imaging due to the unique characteristics of excitation and emission in this region. Near-IR emitting fluorophores use exciting lasers that do not readily cause cellular autofluorescence[1] and are generally noninvasive toward biological samples.[2] These types of fluorophores have found no shortage of uses, including super-resolution microscopy,[3–5] bioimaging and staining,[6–8] and as cellular activity-based probes.[9–12] Selected xanthene-based far-red emitting fluorophores are shown in Figure 1. These include the rhodamine-derived Alexa Fluor 633 (**1**),[13] the carbopyronine Carboxy ATTO 647N (**2**),[14] and the Si-rhodamine Janelia Fluor 646 (**3**).[15] These compounds demonstrate that despite varied scaffolds, organic compounds possessing delocalized electron density can fluoresce in the far-red region.

All of the compounds in Figure 1 are based on the xanthene scaffold.[16] First reported in 2003,[13] the rhodamine dye Alexa Fluor 633 (**1**) dates back to the original *N,N,N′,N′*-tetramethylrhodamine scaffold reported by Ceresole in 1887.[17] Compared with its TMR ancestor, **1** is red-shifted due to altered electronics with sulfonate groups giving it improved aqueous solubility. Changing the rhodamine core oxygen to a quaternary carbon atom, as in **2**, gives rise to carbopyronines dyes. These possess a bathochromic shift relative to rhodamine and were first disclosed in the patent literature by Drexhage et al.[18] ATTO-TEC GmbH have since optimized the photophysics of these dyes with the ATTO 647N fluorophore being based on julolidine and quinoline scaffolds and providing an ideal fluorophore for biological labeling. Substitution of the core oxygen of rhodamine with silicon was first demonstrated as recently as 2008 by Xu et al. to make Si-pyronines with red-shifted fluorescence.[19] The

bathochromic shift in wavelength is proposed to be from LUMO lowering by silicon. Numerous Si-rhodamine probes have been reported by Nagano and coworkers[20–23] as well as the Lavis lab in their recent efforts that demonstrated using azetidine for improved fluorescence properties by minimizing twisted intramolecular charge transfer (TICT) states.[3,15]

All of the fluorophores shown in Figure 1 possess impressive fluorescent properties for imaging, including high photostability, high fluorescent quantum yields, and minimal intersystem crossing to a dark triplet state.[24–26] However, we have found that **2** possesses the unique characteristic of near-total fluorescence stability to organic acid and base. In a recently developed single-molecule peptide sequencing scheme that uses total internal reflection fluorescent microscopy (TIRF) and Edman degradation chemistry, we prepared peptides labeled with ATTO 647N and tested their stabilities to the harsh Edman chemistry, repeated treatment with trifluoroacetic acid (TFA) and pyridine/phenylisothiocyanate (PITC) for up to 20 h.[27] In a solid-phase bead assay, we subjected fluorophores to neat TFA and separately to 9:1 pyridine:PITC both at 40 °C for 24 h. ATTO 647N showed minimal (<5%) changes in fluorescence following subjection to these harsh conditions.[28] This unique characteristic, along with its photophysical properties, make it an ideal fluorophore for these peptide sequencing studies. Additionally, other groups have found this fluorophore to be useful in applications such as Förster resonance energy transfer (FRET) studies and single-molecule imaging,[29–31] enzyme monitoring and protein
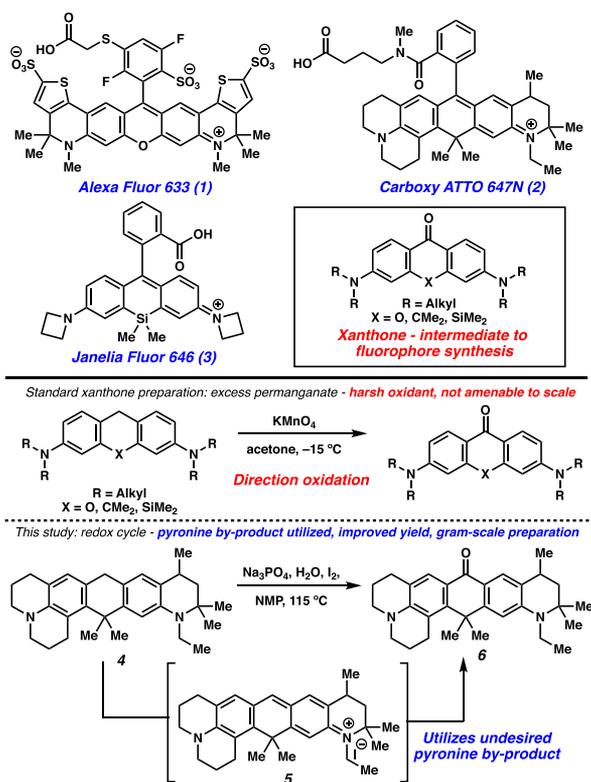
Figure 1. Far-red fluorophores and xanthone synthesis.

conformation,[32,33] lithography,[34] neuron and protein analysis,[35,36] and DNA origami visualization.[37]

A common approach to access the fluorophores shown in Figure 1 is through a xanthone intermediate. Most commonly, substitution of this ketone with an aryl-lithium species gives rise to the conjugated fluorophore,[3,14,38] though other routes have been demonstrated.[39] The standard methodology applied for xanthone synthesis is through direct oxidation of the xanthene with potassium permanganate at reduced temperature.[6,38,40] This oxidation can be challenging for certain scaffolds due to the harsh nature of the oxidant, giving rise to overoxidation and decomposition of the xanthone. Further, the reaction suffers intolerance to many functional groups and is often difficult in increasing reaction scale. As an alternative oxidation, and to highlight the utility of our recently reported redox cycle for xanthone synthesis, we set out to apply this toward the synthesis of xanthone **6**, which takes advantage of the, for most syntheses, undesired pyronine species, e.g. **5**.[41] This comes from spontaneous aerobic oxidation of **4** and cannot be converted directly to **6** by permanganate. We demonstrate gram-scale preparation of **6** in route to Carboxy ATTO 647N (**2**), which was also a valuable target for our group's use in biological imaging. With the ubiquitous use of this fluorophore by the scientific community, the lack of reported literature synthesis, and as a perfect scaffold to demonstrate our recently reported oxidation methodology, we developed a practical procedure for the preparation of Carboxy ATTO 647N (**2**) on a synthetically useful scale.

Carboxy ATTO 647N (2) Retrosynthetic Analysis

To achieve the synthesis of **2** from commercially available starting materials, we relied on precedent for structurally similar carbopyronine fluorophores established by Hell and coworkers.[14]

Scheme 1. Retrosynthetic Analysis of Carboxy ATTO 647N
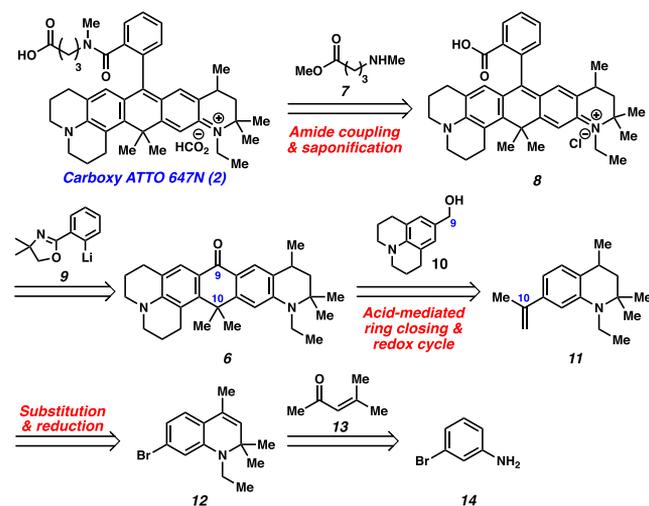
Our retrosynthetic analysis (Scheme 1) is dependent on amide coupling of the benzoic acid derivative **8** with methyl 4-(methylamino)butanoate **7**, followed by saponification of the methyl ester. Acid **8** is derived from ketone **6** following carbonyl substitution at the C9 ketone of the xanthene ring by lithiated aryl oxazole **9** (Scheme 2) and subsequent hydrolysis. The key intermediate, xanthone **6**, was derived from the coupling of julolidine alcohol **10** with tetrahydroquinoline **11**.

Scheme 2. Preparation of Julolidine Fragment 9
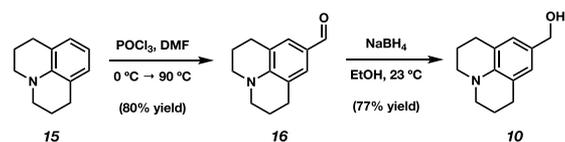
Lewis-acid mediated electrophilic aromatic substitution (EAS) forges the top connection of the molecule, followed by Brønsted acid-promoted EAS to generate quaternary C10. Oxidation of this polycyclic intermediate is accomplished by our recently reported water oxidation cycle using iodine as a terminal oxidant.[41] Tetrahydroquinoline **11** is derived from dihydroquinoline **12** following lithiation of the bromine and substitution onto acetone, which was succeeded by olefin reduction. Dihydroquinoline **12** is accessed from 3-bromoaniline (**14**) by first condensing it with mesityl oxide (**13**) with iodine followed by amine alkylation with Meerwein's reagent. The key xanthone intermediate is accessed on a 1 g scale with preparation of the title compound **2** in over 50 mg batches from only 100 mg of xanthone.

Synthesis of Xanthone Fragments 10 and 11

To initiate our forward synthetic route toward the julolidine alcohol **10** (Scheme 3), julolidine **15** was subjected to Vilsmeier−Haack conditions of phosphorus oxychloride (POCl₃) in N,N-dimethylformamide (DMF) to yield aldehyde **16**.[42] Reduction of the aldehyde with sodium borohydride afforded the julolidine benzyl alcohol **10**, which was highly photosensitive and used rapidly following purification.

In the forward synthetic route to tetrahydroquinoline **11**, the 1,2-dihydroquinoline **17** was prepared from 3-bromoaniline (**14**) by condensation with mesityl oxide (**13**), promoted by iodine, as described by Nagano and coworkers.[21] Ethylation of

Scheme 3. Preparation of Quinoline Fragment 10
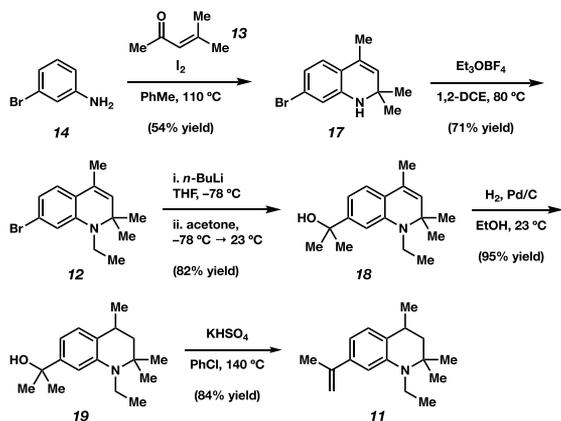
the quinoline nitrogen was accomplished using Meerwein's reagent, triethyloxonium tetrafluoroborate (Et_3OBF_4). This was generated by stirring epichlorohydrin and BF_3OEt_2 in diethyl ether at reflux.[43] After decanting and briefly drying the Meerwein salt, it was heated in 1,2-dichloroethane with quinoline 17. Alkylation proceeded to give quinoline 12 in 71% yield. The aryl bromide was converted to tertiary alcohol 18 by lithiation with n-butyllithium at −78 °C followed by addition of acetone.[6]

To access the tetrahydroquinoline moiety, previous studies showed reduction of the olefin at the aryl bromide stage, as in 17, by hydrogenation required 1 MPa H_2 and heating at 130 °C.[44] For the benzylic alcohol-substituted quinoline 18, it was pleasantly observed that reduction proceeded at ambient temperature with 1 atm of H_2 using 10% wt. Pd/C to yield 1,2,3,4-tetrahydroquinoline 19 in 95% yield. Dehydration of the benzyl alcohol was achieved by treatment with potassium bisulfate ($KHSO_4$) in toluene at reflux,[14] giving the second coupling partner in the synthesis of ketone 6.

Synthesis of Xanthone 6 by Redox Cycling

The key fragment coupling step was accomplished by combining 10 and 11 with the Lewis acid boron trichloride (BCl_3) in methylene chloride at −78 °C, promoting EAS and forging the linkage at C9 (Scheme 4). This was followed by addition of the organic solution to hot phosphoric acid, which was then heated at 115 °C for 3 h to generate carbopyronine xanthene 4.[7] When attempted on the gram scale, oxidation of

xanthene 4 with potassium permanganate ($KMnO_4$) at −15 °C in acetone, the most common methodology for the desired reaction,[6,12,36,38] ketone 6 was isolated in only 18% yield for the 2-step process. It was observed that during the reaction work up after phosphoric acid treatment, 10−20% of 5 was formed due to aerobic oxidation. As Franketszo first showed[18] and further observed by Klán[6] and Hell,[14] oxidation of an analogous xanthene to pyronine (e.g., 4 → 5) proceeds spontaneously under ambient conditions. With the presence of this side-reaction, byproduct 5 cannot participate in oxidation by $KMnO_4$ and thus lowers the overall efficiency of the desired reaction.

To incorporate this unreactive material into the reaction, we applied our recently reported xanthone methodology, which works on both the xanthene and pyronine forms of xanthene-based dyes.[31] Following ring-closing to generate xanthene 4, the crude material was subjected to iodine in N-methyl-2-pyrrolidine (NMP) at room temperature. Within seconds, formation of 5 was apparent as the solution turned a deep blue. To this solution was added sodium phosphate and water, which was then stirred at 115 °C for 8 h and then overnight. The mechanism proceeds by a base-catalyzed conjugate addition of water to the pyronine. Deprotonation of the resulting alcohol results in transfer of a hydride, oxidizing the hydride donor to ketone 6. The hydride acceptor in solution is another molecule of pyronine 5, which accepts the result of the disproportionation and is reduced back to xanthene 4, recycling it and allowing for the oxidation to occur once more. Each molecule of pyronine is split into ketone and xanthene in a 1:1 ratio. At this step in the cycle, iodine oxidizes the xanthene 4 back to pyronine 5, thus driving the cycle forward.[41] Following workup and purification, nearly one gram of ketone 6 was isolated, more than doubling the literature standard methodology.

Late Stage Carboxy ATTO 647N (2) Synthesis

With the synthesis of 6 established, the next step was installation of the aryl group by lithiation and ketone substitution on C9 of the xanthone core. To proceed through this route, masking of benzoic acid 21 was necessary for the strongly basic conditions.

The carboxylic acid 21 was first converted to an acid chloride by treatment with thionyl chloride and catalytic DMF (Scheme 5). The activated acid was added to a solution of 2-

Scheme 4. Synthesis of Xanthone 6 by Redox Cycling
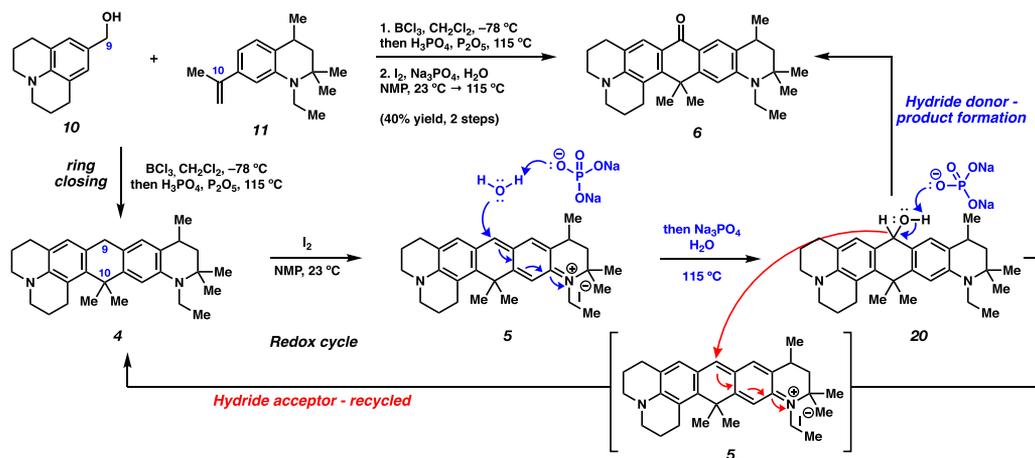
amino-2-methylpropanol with *N*,*N*-diisopropylethylamine (DIPEA) in methylene chloride, forming the primary amide **22**, which was isolated without purification. Again, treatment of the primary amide with thionyl chloride at ambient conditions afforded oxazole **23**.[45]

Scheme 5. Masking Benzoic Acid 21
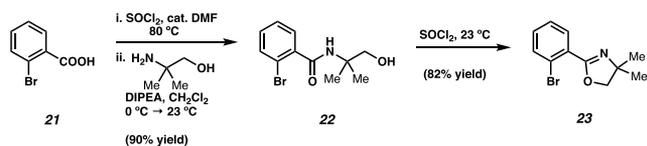
This protected aryl bromide **23** is converted to the aryl lithium species in THF at −78 °C with *t*-BuLi (1.7 M) (Scheme 6). A solution of ketone **6** with the additive *N*,*N*,*N*′,*N*′-tetramethyethylenediamine (TMEDA) was slowly added to the lithiated compound in several portions and stirred overnight. After work up, the aryl oxazole was subjected to heating with 6 N HCl to hydrolyze the oxazole, giving the benzoic acid derivative **8** in a 54% yield over two steps.

Scheme 6. Substitution and Amide Coupling to Give 2
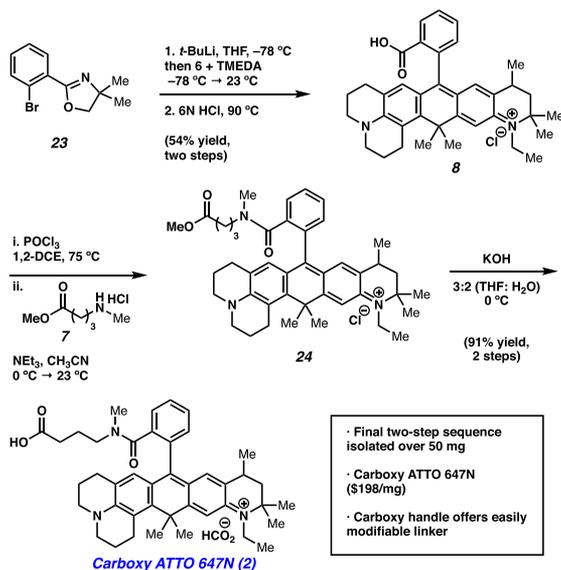
To finish out the synthesis, amide coupling of the acid with amine **7** was carried out by first generating the acid chloride with the use of POCl$_3$; the crude acid chloride was added to a basic solution of **7**, generating the methyl ester **24**. Based on the conditions described by Hell,[14] it was found that methyl ester saponification could be accomplished in very mild conditions with 5 equiv of KOH in a mixture of THF and water (2:1) at 0 °C. Carboxy ATTO 647N (**2**) was isolated by reverse-phase preparative HPLC, as the formate salt of the charged fluorophore in 91% yield for the 2-step amidation and saponification.

In summary, we developed and optimized a straightforward synthesis to the complex fluorophore Carboxy ATTO 647N (**2**). This procedure relies on a new redox methodology for the preparation of the key xanthone intermediate on the mmol scale. We expect that this protocol will increase access and use of the fluorophore and offers a convenient platform to rapidly construct other derivatives of this fluorophore.

■ ASSOCIATED CONTENT

Ⓢ Supporting Information

The Supporting Information is available free of charge at https://pubs.acs.org/doi/10.1021/acs.orglett.9b03981.

    Characterization data including ^{1}H and ^{13}C NMR spectra and high-resolution mass spectral data are given for all compounds as well as full elucidation of all reactions discussed in this text (PDF)

■ AUTHOR INFORMATION

Corresponding Author

*E-mail: anslyn@austin.utexas.edu.

ORCID Ⓞ

Eric V. Anslyn: 0000-0002-5137-8797

Notes

The authors declare the following competing financial interest(s): E.V.A. and E.M.M. are both cofounders and scientific advisory board members of Eryison, Inc.

■ REFERENCES

(1) Guo, Z.; Park, S.; Yoon, J.; Shin, I. Recent progress in the development of near-infrared fluorescent probes for bioimaging applications. *Chem. Soc. Rev.* **2014**, *43* (1), 16−29.

(2) Escobedo, J. O.; Rusin, O.; Lim, S.; Strongin, R. M. NIR dyes for bioimaging applications. *Curr. Opin. Chem. Biol.* **2010**, *14* (1), 64−70.

(3) Grimm, J. B.; Klein, T.; Kopek, B. G.; Shtengel, G.; Hess, H. F.; Sauer, M.; Lavis, L. D. Synthesis of a Far-Red Photoactivatable Silicon-Containing Rhodamine for Super-Resolution Microscopy. *Angew. Chem., Int. Ed.* **2016**, *55* (5), 1723−1727.

(4) Butkevich, A. N.; Mitronova, G. Y.; Sidenstein, S. C.; Klocke, J. L.; Kamin, D.; Meineke, D. N. H.; D'Este, E.; Kraemer, P.-T.; Danzl, J. G.; Belov, V. N.; Hell, S. W. Fluorescent Rhodamines and Fluorogenic Carbopyronines for Super-Resolution STED Microscopy in Living Cells. *Angew. Chem., Int. Ed.* **2016**, *55* (10), 3290−3294.

(5) Butkevich, A. N.; Belov, V. N.; Kolmakov, K.; Sokolov, V. V.; Shojaei, H.; Sidenstein, S. C.; Kamin, D.; Matthias, J.; Vlijm, R.; Engelhardt, J.; Hell, S. W. Hydroxylated Fluorescent Dyes for Live-Cell Labeling: Synthesis, Spectra and Super-Resolution STED. *Chem. - Eur. J.* **2017**, *23* (50), 12114−12119.

(6) Pastierik, T.; Šebej, P.; Medalová, J.; Štacko, P.; Klán, P. Near-Infrared Fluorescent 9-Phenylethynylpyronin Analogues for Bioimaging. *J. Org. Chem.* **2014**, *79* (8), 3374−3382.

(7) Lukinavičius, G.; Blaukopf, C.; Pershagen, E.; Schena, A.; Reymond, L.; Derivery, E.; Gonzalez-Gaitan, M.; D'Este, E.; Hell, S. W.; Wolfram Gerlich, D.; Johnsson, K. SiR−Hoechst is a far-red DNA stain for live-cell nanoscopy. *Nat. Commun.* **2015**, *6*, 8497.

(8) Chai, X.; Cui, X.; Wang, B.; Yang, F.; Cai, Y.; Wu, Q.; Wang, T. Near-Infrared Phosphorus-Substituted Rhodamine with Emission Wavelength above 700 nm for Bioimaging. *Chem. - Eur. J.* **2015**, *21* (47), 16754−16758.

(9) Brewer, T. F.; Chang, C. J. An Aza-Cope Reactivity-Based Fluorescent Probe for Imaging Formaldehyde in Living Cells. *J. Am. Chem. Soc.* **2015**, *137* (34), 10886−10889.

(10) Chang, M. C. Y.; Pralle, A.; Isacoff, E. Y.; Chang, C. J. A Selective, Cell-Permeable Optical Probe for Hydrogen Peroxide in Living Cells. *J. Am. Chem. Soc.* **2004**, *126* (47), 15392−15393.

(11) Nolan, E. M.; Lippard, S. J. A "Turn-On" Fluorescent Sensor for the Selective Detection of Mercuric Ion in Aqueous Media. *J. Am. Chem. Soc.* **2003**, *125* (47), 14270−14271.

(12) Yang, Y.; Seidlits, S. K.; Adams, M. M.; Lynch, V. M.; Schmidt, C. E.; Anslyn, E. V.; Shear, J. B. A Highly Selective Low-Background Fluorescent Imaging Agent for Nitric Oxide. *J. Am. Chem. Soc.* **2010**, *132* (38), 13114−13116.

(13) Berlier, J. E.; Rothe, A.; Buller, G.; Bradford, J.; Gray, D. R.; Filanoski, B. J.; Telford, W. G.; Yue, S.; Liu, J.; Cheung, C.-Y.; Chang, W.; Hirsch, J. D.; Beechem Rosaria, P.; Haugland, J. M.; Haugland, R. P. Quantitative Comparison of Long-wavelength Alexa Fluor Dyes to Cy Dyes: Fluorescence of the Dyes and Their Bioconjugates. *J. Histochem. Cytochem.* **2003**, *51* (12), 1699−1712.

(14) Kolmakov, K.; Belov, V. N.; Wurm, C. A.; Harke, B.; Leutenegger, M.; Eggeling, C.; Hell, S. W. A Versatile Route to Red-Emitting Carbopyronine Dyes for Optical Microscopy and Nanoscopy. *Eur. J. Org. Chem.* **2010**, *2010* (19), 3593−3610.

(15) Grimm, J. B.; Brown, T. A.; Tkachuk, A. N.; Lavis, L. D. General Synthetic Method for Si-Fluoresceins and Si-Rhodamines. *ACS Cent. Sci.* **2017**, *3* (9), 975−985.

(16) Beija, M.; Afonso, C. A. M.; Martinho, J. M. G. Synthesis and applications of Rhodamine derivatives as fluorescent probes. *Chem. Soc. Rev.* **2009**, *38* (8), 2410−2433.

(17) Ceresole, M. *Verfahren zur Darstellung von Farbstoffen aus der Gruppe des Meta-amidophenolphtaleïns*; 1887.

(18) Drexhage, K.-H.; Arden-Jacob, J.; Frantzeskos, J.; Zilles, A. Carbopyronine fluorescent dyes. US6828159B1, 1999.

(19) Fu, M.; Xiao, Y.; Qian, X.; Zhao, D.; Xu, Y. A design concept of long-wavelength fluorescent analogs of rhodamine dyes: replacement of oxygen with silicon atom. *Chem. Commun.* **2008**, *15*, 1780−1782.

(20) Koide, Y.; Urano, Y.; Hanaoka, K.; Terai, T.; Nagano, T. Evolution of Group 14 Rhodamines as Platforms for Near-Infrared Fluorescence Probes Utilizing Photoinduced Electron Transfer. *ACS Chem. Biol.* **2011**, *6* (6), 600−608.

(21) Koide, Y.; Urano, Y.; Hanaoka, K.; Piao, W.; Kusakabe, M.; Saito, N.; Terai, T.; Okabe, T.; Nagano, T. Development of NIR Fluorescent Dyes Based on Si−rhodamine for in Vivo Imaging. *J. Am. Chem. Soc.* **2012**, *134* (11), 5029−5031.

(22) Terai, T.; Nagano, T. Small-molecule fluorophores and fluorescent probes for bioimaging. *Pfluegers Arch.* **2013**, *465* (3), 347−359.

(23) Hanaoka, K.; Kagami, Y.; Piao, W.; Myochin, T.; Numasawa, K.; Kuriki, Y.; Ikeno, T.; Ueno, T.; Komatsu, T.; Terai, T.; Nagano, T.; Urano, Y. Synthesis of unsymmetrical Si-rhodamine fluorophores and application to a far-red to near-infrared fluorescence probe for hypoxia. *Chem. Commun.* **2018**, *54* (50), 6939−6942.

(24) van der Velde, J. H. M.; Oelerich, J.; Huang, J.; Smit, J. H.; Aminian Jazi, A.; Galiani, S.; Kolmakov, K.; Gouridis, G.; Eggeling, C.; Herrmann, A.; Roelfes, G.; Cordes, T. A simple and versatile design concept for fluorophore derivatives with intramolecular photostabilization. *Nat. Commun.* **2016**, *7*, 10144.

(25) Grimm, J. B.; English, B. P.; Chen, J.; Slaughter, J. P.; Zhang, Z.; Revyakin, A.; Patel, R.; Macklin, J. J.; Normanno, D.; Singer, R. H.; Lionnet, T.; Lavis, L. D. A general method to improve fluorophores for live-cell and single-molecule microscopy. *Nat. Methods* **2015**, *12*, 244.

(26) Moreira, B. G.; You, Y.; Owczarzy, R. Cy3 and Cy5 dyes attached to oligonucleotide terminus stabilize DNA duplexes: Predictive thermodynamic model. *Biophys. Chem.* **2015**, *198*, 36−44.

(27) Swaminathan, J.; Boulgakov, A. A.; Hernandez, E. T.; Bardo, A. M.; Bachman, J. L.; Marotta, J.; Johnson, A. M.; Anslyn, E. V.; Marcotte, E. M. Highly parallel single-molecule identification of proteins in zeptomole-scale mixtures. *Nat. Biotechnol.* **2018**, *36*, 1076.

(28) Laursen, R. A. Solid-Phase Edman Degradation. *Eur. J. Biochem.* **1971**, *20* (1), 89−102.

(29) Roth, D. J.; Nasir, M. E.; Ginzburg, P.; Wang, P.; Le Marois, A.; Suhling, K.; Richards, D.; Zayats, A. V. Förster Resonance Energy Transfer inside Hyperbolic Metamaterials. *ACS Photonics* **2018**, *5* (11), 4594−4603.

(30) Kim, J.-y.; Kim, C.; Lee, N. K. Real-time submillisecond single-molecule FRET dynamics of freely diffusing molecules with liposome tethering. *Nat. Commun.* **2015**, *6*, 6992.

(31) Xin, L.; Lu, M.; Both, S.; Pfeiffer, M.; Urban, M. J.; Zhou, C.; Yan, H.; Weiss, T.; Liu, N.; Lindfors, K. Watching a Single Fluorophore Molecule Walk into a Plasmonic Hotspot. *ACS Photonics* **2019**, *6* (4), 985−993.

(32) Lunau, N.; Seelhorst, K.; Kahl, S.; Tscherch, K.; Stacke, C.; Rohn, S.; Thiem, J.; Hahn, U.; Meier, C. Fluorescently Labeled Substrates for Monitoring α1,3-Fucosyltransferase IX Activity. *Chem. - Eur. J.* **2013**, *19* (51), 17379−17390.

(33) Sánchez-Rico, C.; Voith von Voithenberg, L.; Warner, L.; Lamb, D. C.; Sattler, M. Effects of Fluorophore Attachment on Protein Conformation and Dynamics Studied by spFRET and NMR Spectroscopy. *Chem. - Eur. J.* **2017**, *23* (57), 14267−14277.

(34) Vijayamohanan, H.; Bhide, P.; Boyd, D.; Zhou, Z.; Palermo, E. F.; Ullal, C. K. Effect of Chemical Microenvironment in Spirothiopyran Monolayer Direct-Write Photoresists. *Langmuir* **2019**, *35* (11), 3871−3879.

(35) Meissner, G. W.; Grimm, J. B.; Johnston, R. M.; Sutcliffe, B.; Ng, J.; Jefferis, G. S. X. E.; Cachero, S.; Lavis, L. D.; Malkesman, O. Optimization of fluorophores for chemical tagging and immunohistochemistry of Drosophila neurons. *PLoS One* **2018**, *13* (8), e0200759.

(36) Yao, J. Z.; Uttamapinant, C.; Poloukhtine, A.; Baskin, J. M.; Codelli, J. A.; Sletten, E. M.; Bertozzi, C. R.; Popik, V. V.; Ting, A. Y. Fluorophore Targeting to Cellular Proteins via Enzyme-Mediated Azide Ligation and Strain-Promoted Cycloaddition. *J. Am. Chem. Soc.* **2012**, *134* (8), 3720−3728.

(37) Stein, I. H.; Steinhauer, C.; Tinnefeld, P. Single-Molecule Four-Color FRET Visualizes Energy-Transfer Paths on DNA Origami. *J. Am. Chem. Soc.* **2011**, *133* (12), 4193−4195.

(38) Butkevich, A. N.; Ta, H.; Ratz, M.; Stoldt, S.; Jakobs, S.; Belov, V. N.; Hell, S. W. Two-Color 810 nm STED Nanoscopy of Living Cells with Endogenous SNAP-Tagged Fusion Proteins. *ACS Chem. Biol.* **2018**, *13* (2), 475−480.

(39) Calitree, B. D.; Detty, M. R. *Novel Rhodamine Dyes via Suzuki Coupling of Xanthone Triflates with Arylboroxins*. 2010; Vol. *41*. DOI: 10.1002/chin.201019176

(40) Shieh, P.; Dien, V. T.; Beahm, B. J.; Castellano, J. M.; Wyss-Coray, T.; Bertozzi, C. R. CalFluors: A Universal Motif for Fluorogenic Azide Probes across the Visible Spectrum. *J. Am. Chem. Soc.* **2015**, *137* (22), 7145−7151.

(41) Bachman, J. L.; Escamilla, P. R.; Boley, A. J.; Pavlich, C. I.; Anslyn, E. V. Improved Xanthone Synthesis, Stepwise Chemical Redox Cycling. *Org. Lett.* **2019**, *21* (1), 206−209.

(42) Cai, G.; Bozhkova, N.; Odingo, J.; Berova, N.; Nakanishi, K. Circular dichroism exciton chirality method. New red-shifted chromophores for hydroxyl groups. *J. Am. Chem. Soc.* **1993**, *115* (16), 7192−7198.

(43) Meerwein, H. Triethyloxonium Fluoborate. *Organic Syntheses* **1966**, *46*, 113.

(44) Chen, R.; Yang, X.; Tian, H.; Wang, X.; Hagfeldt, A.; Sun, L. Effect of Tetrahydroquinoline Dyes Structure on the Performance of Organic Dye-Sensitized Solar Cells. *Chem. Mater.* **2007**, *19* (16), 4007−4015.

(45) Lukinavičius, G.; Umezawa, K.; Olivier, N.; Honigmann, A.; Yang, G.; Plass, T.; Mueller, V.; Reymond, L.; Corrêa, I. R., Jr; Luo, Z.-G.; Schultz, C.; Lemke, E. A.; Heppenstall, P.; Eggeling, C.; Manley, S.; Johnsson, K. A near-infrared fluorophore for live-cell super-resolution microscopy of cellular proteins. *Nat. Chem.* **2013**, *5*, 132.